J Mater Sci: Mater Med (2009) 20:949–957
DOI 10.1007/s10856-008-3645-5

Preparation and HL-7702 cell functionality of titania/chitosan composite scaffolds

Li Zhao · Jiang Chang · Wanyin Zhai

Received: 22 August 2008 / Accepted: 3 November 2008 / Published online: 26 November 2008

Abstract Titania/chitosan composite scaffolds were prepared through a freeze-drying technique. The composite scaffolds were highly porous with the average pore size of 120–300 μm, and the titania (TiO_2) powders were uniformly dispersed on the surface of the pore walls. The compressive strength of the composite scaffolds was significantly improved compared to that of pure chitosan scaffolds. Composite scaffold with 0.3 of TiO_2/chitosan weight ratio showed the maximum compressive strength of 159.7 ± 21 kPa. Hepatic immortal cell line HL-7702 was used as seeding cells on the scaffolds, and after different culture periods, cell attachment and function was analyzed. HL-7702 cells attached on the pore walls of the scaffolds with the spheroid shape after 1 day of culture, but more cell aggregations formed within the TiO_2/chitosan composite scaffolds as compared to pure chitosan scaffolds. Liver-specific functions, albumin secretion and urea synthesis were detected using a spectrometric method. The results showed that albumin secretion and urea synthesis rate of HL-7702 cells slightly decreased with the culture time, and there was no significant difference between composite scaffolds and pure chitosan scaffolds. In conclusion, the TiO_2/chitosan composite scaffolds possessed an improved mechanical strength compared to pure chitosan scaffolds and supported the attachment and functional expression of hepatocyte, implying their potential application in liver tissue engineering.

L. Zhao (✉)
Shanghai Tissue Engineering Research and Development Center, Shanghai, China
e-mail: zl3578@126.com

J. Chang · W. Zhai
Biomaterials and Tissue Engineering Research Center, Shanghai Institute of Ceramics, Chinese Academy of Sciences, Shanghai, China

1 Introduction

In the past 30 years, many researchers have demonstrated that it was difficult to develop extracorporeal culture system of hepatocytes mimicking in vivo microenvironment. The main obstacle is the loss of hepatocytes biological viability and the deviation of differentiation function [1]. The optimal condition for hepatocyte culture is to organize three-dimension (3D) spatial microenvironment similar to in vivo alive surroundings. Constructing macroporous scaffolds in vitro allows cell–cell contact resulting in the formation of multicellular organism. In vivo, most of cells are surrounded by congenetic or different embryonic cells, thus it could be believed that cell–cell contact is beneficial for cell growth in vitro [2]. The choice of appropriate materials for the preparation of scaffolds is of importance for in vitro hepatocyte culture and the maintenance of metabolic function.

Many investigators have proposed porous biodegradable, as well as non-degradable polymeric scaffolds for tissue-engineering applications. Examinations using all these scaffolds indicated an interaction between the scaffold architecture and the cell culture. However, existing scaffolds are considered to be less than ideal in terms of high-density cultures of hepatocytes maintaining long-term metabolic functions. To this end, the research on 3D scaffolds for hepatocyte culture has been largely confined to designing matrices made of synthetic polymers such as poly(lactide-co-glycolide) (PLGA) [3, 4], or from the natural extracellular matrix (ECM) components, such as the

two-layer collagen gels [5] and EHS gels (ECM prepared from the Engelberth-Holm Swarm mouse sarcoma) [6]. Hepatocytes cultured within the PLGA scaffolds (foams or sponges) retained viability; however, their liver-specific gene expression was limited [7]. Some research even demonstrated that in artificial liver system, PLGA was lack of biocompatibility with cells and bloods. For example, 90–95% of the hepatocytes died within 24 h after implantation in a PLGA scaffold [8]. In contrast, hepatocytes seeded within the natural ECM-derived scaffolds maintained their differentiated function for prolonged times [5]. A major limitation of ECM-derived systems, in particular those made from EHS, is their potential antigenicity and tumoregenicity when the material is implanted into a host [9]. Lim et al. reported that encapsulation of cells into alginate capsules (AC) could produce a very high-density cell culture system with mechanical support to the cells as well as immunoprotection in the event of implantation [10]. However, hepatocytes encapsulated in AC are of low viability and do not maintain the long-term liver functions due to the lack of cell–matrix and cell–cell interactions within AC [11, 12]. Therefore, it is urgent to develop a suitable substrate for optimal hepatocyte attachment and long-term function maintenance.

In this study, chitosan was selected for hepatocytes attachment because chitosan is a linear polysaccharide consisting of $\beta(1 \rightarrow 4)$ linked D-glucosamine residues with a variable number of randomly located N-acetyl-glucosamine groups, which are similar to glycosaminoglycans, the components of extracellular matrix [13]. Kawase et al. indicated that chitosan component, owing to its analogy to natural hepatic matrix, may play an important role in maintaining the differentiated liver functions [14]. Galactosylated chitosan [15] and fructose-modified chitosan [16] scaffolds both promoted the formation of cellular aggregates, exhibiting spherical shape of hepatocytes. However, the natural polymer is mechanically weak, which limits its biomedical application.

Previous studies revealed that TiO_2 thin films were shown to be the optimal surface for the faster attachment compared with other kinds of nanoparticle thin films [17]. In our previous research, hepatocytes had good affinity for anatase and rutile ceramics and TiO_2 could stimulate cell proliferation to a certain extent [18]. The findings of Buchloh et al. suggested that around 90% of all cells attached to the titanium dioxide surfaces exhibiting a spherical morphology and hepatocytes did not recognize the specific differences of differently orientated rutile crystal surfaces [19]. In addition, TiO_2 incorporation into the high-density polyethylene (HDPE) matrix effectively enhanced the mechanical strength of HDPE [20]. Therefore, it is speculated that the incorporation of TiO_2 particles into chitosan scaffolds will improve their mechanical strength and further maintain a long-term functionality. In this study, the effect of TiO_2 in chitosan scaffolds on their mechanical and biological properties was investigated.

2 Materials and method

2.1 Preparation of TiO_2/chitosan composite scaffolds

Chitosan was dissolved in 0.2 M acetic acid aqueous solution to obtain the solution with the concentration of 2 wt%. TiO_2 powders was prepared by $TiCl_4$ hydrolysis [18] and Fig. 1 shows the transmission electron micrograph (TEM) of TiO_2 powder calcined at 500°C. The vast majority of particles are rodlike and the size distribution of particles was in the range of 25–75 nm. TiO_2 powders were added to the prepared chitosan solution according to the weight ratio of TiO_2/chitosan (0, 0.02, 0.05, 0.1, 0.3, 0.5, 0.7), the mixture was stirred overnight at room temperature, and then transferred to a refrigerator at a preset freezing temperature of −20°C to solidify the solvent. The solidified mixture was maintained at the preset temperature for at least 8 h, and then transferred into a freezing-drier and lyophilized. After drying, the samples were neutralized in 1 M NaOH solution for 1 h at room temperature, rinsed using deionized water and lyophilized again. The obtained composite scaffolds were denoted as CT_0, $CT_{0.02}$, $CT_{0.05}$, $CT_{0.1}$, $CT_{0.3}$, $CT_{0.5}$, $CT_{0.7}$. The subscript means the weight ratio of TiO_2/chitosan.

2.2 Characterization of the composite scaffolds

Microstructural characterization of the composite scaffolds was carried out using a Shimadzu 8705QH_2 electron probe microanalyzer (EPMA) (Shimadzu Co., Japan) at an

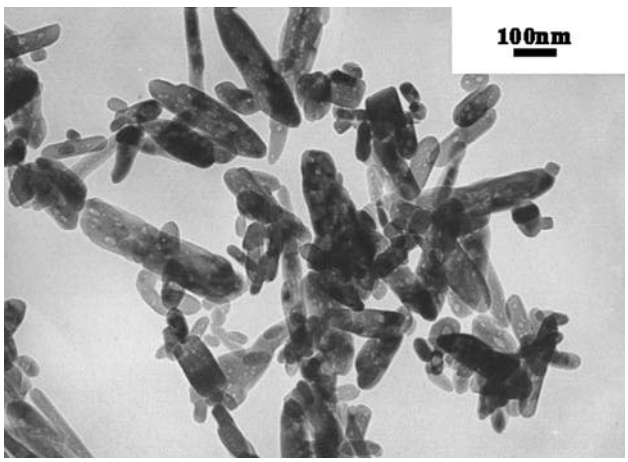

Fig. 1 Transmission electron micrographs of TiO_2 powders calcined at 500°C for 2 h

accelerating voltage of 20 kV. Before observation, the scaffolds were sputter-coated with gold under argon atmosphere. For mechanical testing, the composite scaffolds with the dimension of 8.5 mm in diameter and 10 mm in height were prepared and the compressive strength was conducted using an AG-1 Shimadzu mechanical tester (Shimadzu Co., Japan). The crosshead speed was 0.5 mm/min and the value of the compressive strength was the average of five test results.

The porosities of the composite scaffolds were determined with the liquid displacement method [21, 22].

2.3 Cell culture

A human normally hepatic immortal cell line HL-7702 obtained from Shanghai Cell Biology Institute, Chinese Academy of Sciences, was used in the experiments. The cells were cultured in RPMI 1640 medium supplemented with 10% fetal calf serum (FCS), antibiotics (100 U/ml penicillin, 100 mg/ml streptomycin), and glutamine (200 mM) at 37°C in a humidified atmosphere of 5% CO_2 and 95% air. The cells were regularly subcultured by trypsinization (0.25% w/v, trypsin in D-Hanks sodium with 0.2% EDTA-Na) and the medium was changed every 2 days.

2.4 Cell seeding and attachment on the scaffolds

Before seeding, the scaffolds with the dimension of 5 mm in diameter and 3 mm in height were soaked in 75% alcohol for 40 min, and then exposed to UV light overnight. The scaffolds were placed into the well of 48-well culture plate and cell suspension containing 1×10^6 cells was injected into the scaffolds using a syringe. After attachment for 2 h, 1 ml medium was then added and the cell/scaffold constructs were maintained at 37°C in a humidified 5% CO_2 incubator. After 1 day of culture, the cell/scaffold constructs were transferred to a new culture plate and continued to be incubated with the medium replaced every day. The changed medium were collected and stored in a refrigerator at −20°C for the measurement of hepatocytes function.

Cell attachment efficiency was detected by 3-(4,5-dimethylthiazol-2-yl)-2,5-diphenyl tetrazolium bromide (MTT) assay. MTT was first performed on a directly counted human hepatic HL-7702 cell serial (0.5×10^5, 1.0×10^5, 1.5×10^5, 2.0×10^5 cells/ml), the absorbency values were plotted against the counted cell numbers to establish a standard calibration curve. At the end of 1 day of culture, 15 μl of MTT solution (5 mg ml^{-1}) was added into each well (including wells of the former culture plate), and incubated for 3 h at 37°C/5% CO_2. Then the medium was aspirated and 200 μl of dimethyl sulfoxide (DMSO, Sigma) were added into each well to dissolve the MTT-formazan product. Stirred for 10 min, the solutions were transferred to a new 96-well plate and the optical density was measured spectrophotometricaly at 490 nm by a microplate reader (GMBH A-1160, Dialab, Austria). According to the standard curve, the cell numbers unattached, which were leaked out from the scaffolds and the cell numbers attached on the scaffolds were counted. Cell attachment efficiency was measured according to the following equation:

$$\begin{aligned}&\text{Cell attachment efficiency}(\%)\\&= (\text{Total cell seeding numbers} - \text{cell numbers unattached})\\&\quad /\text{Total cell seeding numbers}\end{aligned}$$

2.5 Cell morphology

After being cultured for 1 day and 7 days, the cellular constructs were harvested, washed with phosphate buffered solution (PBS) to remove non-adherent cells, fixed with 2.5% glutaraldehyde solution at room temperature, dehydrated through a series of graded alcohol solutions, and then exchanged by hexamethydisilanzane (HMDS). After the evaporation of HMDS, the cell morphology was observed by field emission scanning electron microscope (FESEM) (JSM-6700F, JEOL Co., Japan).

2.6 Albumin secretion

During the HL-7702 cells culture period, medium samples were assayed by using a commercial albumin kit (Kehua-Dongling Diagnostic Products Co. Ltd, Shanghai, China). The secretion rate of albumin was determined using a published spectrophotometrical method [16]. The standard pure albumin (40 mg/ml) and samples were added into 2 ml of bromocresol green (BCG). Then, after reaction at 37°C in 60 s, the color change was monitored spectrophotometrically at 630 nm. The absorbance of the standard albumin at the wavelength of 630 nm was used as a control, albumin secretion of hepatocytes in the culture medium was determined according to the following equation:

$$\begin{aligned}&\text{Albumin in the samples (mg/ml)}\\&= \text{Sample absorbance}/\text{Standard liquid absorbance} * 40\end{aligned}$$

2.7 Urea synthesis

Urea levels were determined by the Urea Nitrogen Diagnostic Kit ((Kehua-Dongling Diagnostic Products Co. Ltd, Shanghai, China) that utilizes a urease/Berthelot, quantitative, colorimetric method [23]. Into test tubes were added 20 μl of sample followed by 0.4 ml urease solution, 2 ml

developer A (phenol, sodium nitroferricyanide) and 2 ml developer B (sodium hypochlorite, sodium hydroxide). After gentle mixing, the tubes were allowed to stand at 37°C for 15–20 min while urea hydrolyzed to ammonia. The color change was monitored spectrophotometrically at the wavelength of 550 nm. Sample concentration was determined using a urea nitrogen (7.14 mmol/l) standard liquid according to the following equation:

$$\text{Urea in the samples (mmol/l)} = \text{Sample absorbance}/\text{Standard liquid absorbance} * 7.14$$

2.8 Statistics

Results data were expressed as mean ± standard deviation (SD). The statistical significance between two sets of data was calculated using a Student's *t* test. Difference was considered to be significant when a *P* value of 0.05 or less was obtained (showing a 95% confidence limit).

3 Results

3.1 Microstructure of the composite scaffolds

TiO_2/chitosan composite scaffolds had interconnected porous structure, as shown in Fig. 2. In the pure chitosan scaffold, regular pore structure was observed with the pore size of 80–200 μm (Fig. 2a). With the increase of TiO_2 content, the pore structure of the composite scaffolds became more irregular and the pore size increased. The pore size of $CT_{0.7}$ composite scaffolds varied from 180 μm to 420 μm (Fig. 2d). High magnification SEM images showed that TiO_2 particles dispersed homogenously on the pore walls of the composite scaffolds with lower TiO_2 content (Fig. 3).

The porosities of the composite scaffolds were listed in Table 1. The porosity of the chitosan scaffold was 92.6%. The porosity of the composite scaffolds decreased with the increase of TiO_2 content, while $CT_{0.7}$ composite scaffolds still maintained high porosity of 89.6%.

3.2 Mechanical strength

An additional desirable feature of scaffolds used for tissue engineering is good mechanical properties that will enable them to maintain their shape during in vitro cell culture, during the surgical procedure for transplantation and in the body. Thus, the mechanical properties of the TiO_2/chitosan composite scaffolds were characterized. Figure 4 showed the compressive strength of the composite scaffolds as a function of TiO_2 content at a freezing temperature of −20°C. It is clear to see that the compressive strength of the composite scaffolds increased with the increase of TiO_2 content, reaching the maximum of 159.7 ± 21 kPa when the weight ratio of TiO_2/chitsoan was 0.3, and then decreased with the further increase of TiO_2 content. As compared to the pure chitosan scaffold, the compressive strength of the composite scaffold was significantly improved. Incorporation of TiO_2 into chitosan scaffolds caused a significant enhancement of mechanical properties in the composite scaffolds.

3.3 Cell attachment and morphology within the scaffolds

The interaction of HL-7702 cell line with the scaffolds was first evaluated with checking the initial ability of cells attachment onto the scaffolds. We observed that the TiO_2/chitosan composite scaffolds and the pure chitosan scaffolds were good substrata for HL-7702 cell attachment. The cell attachment efficiency on the chitosan and TiO_2/chitosan composite scaffolds was 75.9% and 81.2%, respectively.

HL-7702 cells within the pores of the scaffolds exhibited a round cellular morphology similar to the cells in vivo after 1 day of culture (Fig. 5). Within the chitosan scaffold, most of cells were single cell with few cell–cell contacts, while within the TiO_2/chitosan composite scaffolds, most of cells formed aggregates within the pores of the scaffolds indicating that the addition of TiO_2 into chitosan caused an increase in cellular interaction that formed cellular aggregates similar to those in vivo. After culturing for 7 days, cells still retained spherical morphology within the chitosan scaffold scattering on the pore walls (Fig. 6a). Within the TiO_2/chitosan composite scaffold, cell aggregations maintained on the pore walls, but single cells were also observed (Fig. 6b).

3.4 Metabolic activities

Metabolic activities were investigated in terms of albumin secretion which was specific to liver and urea synthesis which represented the function of detoxification [1]. Albumin secretion rate of HL-7702 cells within chitosan and TiO_2/chitosan composite scaffolds with culture time was shown in Fig. 7. The results indicated that albumin secretion level reached the highest after culturing for 7 days within the chitosan scaffolds, while at the end of 1 day, albumin secretion rate reached highest within the TiO_2/chitosan composite scaffolds. But, during the culture time for up to 14 days, there was no significant difference between pure chitosan scaffold and composite scaffold. Urea synthesis within the scaffolds also slightly decreased with culture time, and there was also no significant difference between chitosan and TiO_2/chitosan composite scaffolds (Fig. 8).

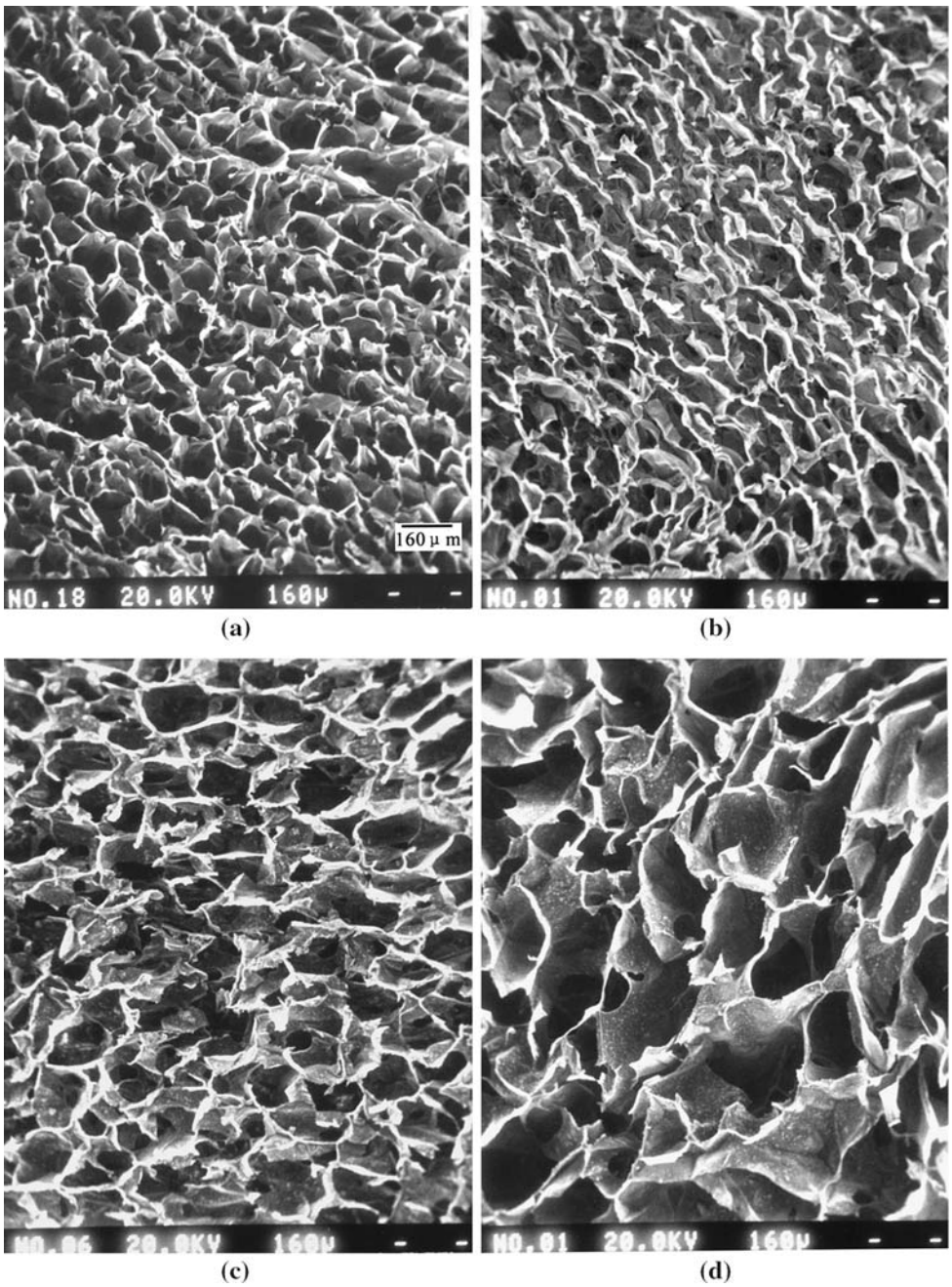

Fig. 2 SEM micrographs of cross section of TiO_2/chitosan composite scaffolds: **a** CT_0; **b** $CT_{0.1}$; **c** $CT_{0.5}$; **d** $CT_{0.7}$

Urea synthesis rate of HL-7702 cells within the scaffolds was at a level of 21–22 μg/10^6 cells/day.

4 Discussion

In this study, TiO_2/chitosan composite scaffolds with a high porosity (>89%) were successfully prepared using a freeze-drying technique. The scaffold possessed a highly porous structure, with an average pore size of 120–300 μm and interconnected pores. During the freeze-drying process, water was homogeneously distributed within the chitosan network containing hydrophilic TiO_2 powder, allowing the latter to enlarge uniformly and the ice crystals to act as porogen.

In liver tissue engineering, scaffolds offer a space for hepatocytes aggregation and mechanical support for retaining hepatocytes long-term metabolic activities. Chitosan is a naturally derived polymer that lacks long-term mechanical stability. So, in this study we attempted to improve the mechanical properties of chitosan scaffolds by focusing on combining it with TiO_2. Our results demonstrated that the addition of TiO_2 powders did not influence the porous structure of the scaffolds, and conversely, led to

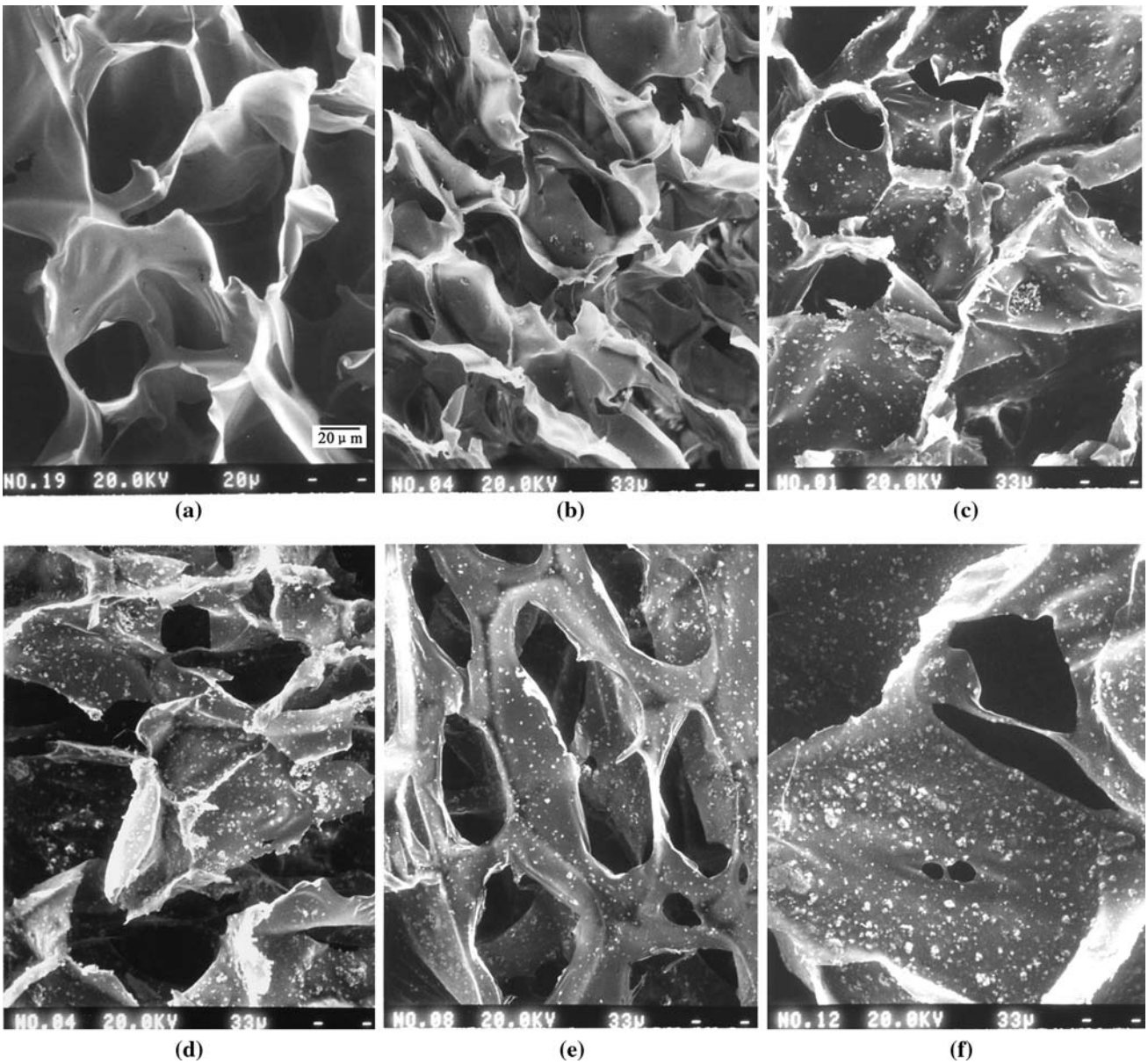

Fig. 3 SEM micrographs of the cross-section of TiO_2/chitosan composite scaffolds with high magnification: **a** CT_0; **b** $CT_{0.1}$; **c** $CT_{0.3}$; **d** $CT_{0.5}$; **e** surface section of $CT_{0.5}$; **f** $CT_{0.7}$

Table 1 Porosities of TiO_2/chitosan composite scaffolds

Samples	TiO_2/chitosan ratio	Freezing temperature (°)	Porosity (%)
CT_0	0	−20	92.6
$CT_{0.1}$	0.1	−20	92.2
$CT_{0.3}$	0.3	−20	91.6
$CT_{0.5}$	0.5	−20	91.7
$CT_{0.7}$	0.7	−20	89.6

a significant improvement in compressive strength. And, $CT_{0.3}$ was the optional composition reaching the maximum compressive strength. Therefore, $CT_{0.3}$ was chosen as the representative composite scaffold for further cellular experiments. The potential reason for the effective enhancement of mechanical strength is that its high surface area of TiO_2 powders improves the interaction and adhesion between polymer and fillers [20]. When the contents of TiO_2 powders are too high, the powders strongly perturb the crystallization of the solvent during the freezing process, which result in the structural integrity being damaged and a dramatic decrease of the mechanical strength taking place. Moreover, with the increase of TiO_2 content, TiO_2 powders exhibited a severe agglomeration tendency, which may cause decreasing compressive strength of the composite scaffold [24].

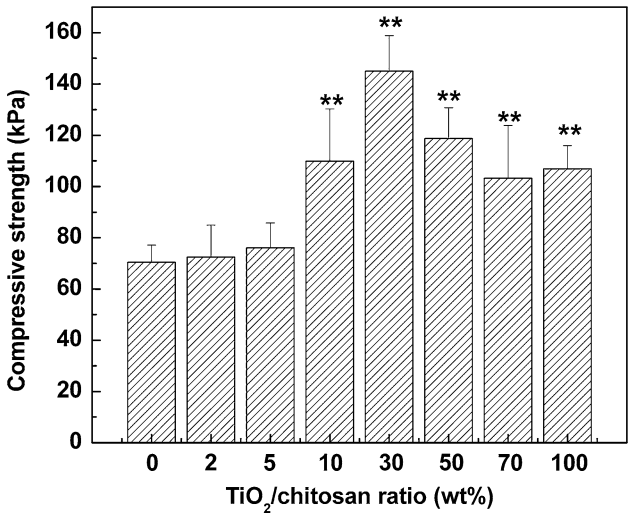

Fig. 4 Compressive strength of TiO_2/chitosan composite scaffolds as a function of TiO_2 content. Each value is the mean ± standard derivation ($n = 3$). **Denotes significant difference compared to chitosan scaffold ($P \leq 0.05$)

According to the theory of particle reinforcement [25], the matrix bears the load in the particle-reinforced composite materials. The particles dispersed uniformly in the matrix, blocking the movement of macromolecule chain of the polymer matrix. The effect of particle reinforcement was related to the volume fraction, uniformity and size of particles in the matrix. When the particle size was in the range of 0.01–0.1 μm, the reinforcement effect was the best. Once the particle size exceeded 0.1 μm, stress concentration occurred. Thus, the compressive strength of TiO_2/chitosan composite scaffolds with lower TiO_2 content could be significantly improved because of a homogeneous dispersion of nanoparticles in a polymeric matrix. When the weight fraction of TiO_2 powders increased, the particle size resulting from particle agglomeration exceeded 0.1 μm, the reinforcement effect weakened and the compressive strength decreased. Likewise, in the composite membrane, the addition of inorganic particles increased the mechanical strength, but when the inorganic particle content continued to increase, the mechanical strength of composite membrane decreased [26].

Some other researchers have found better performance of hepatocyte culture in 3D structures rather than on 2D surfaces [27, 28]. Porous TiO_2/chitosan composite scaffolds in this paper could provide optimal spatial condition for seeding a large cell mass and for nutrition infiltration and metabolic removal. On the other hand, seeding HL-7702 cells into the TiO_2/chitosan composite scaffolds was efficient due to the hydrophilic nature of the chitosan polymer and TiO_2 powder and the rapid wetting of the

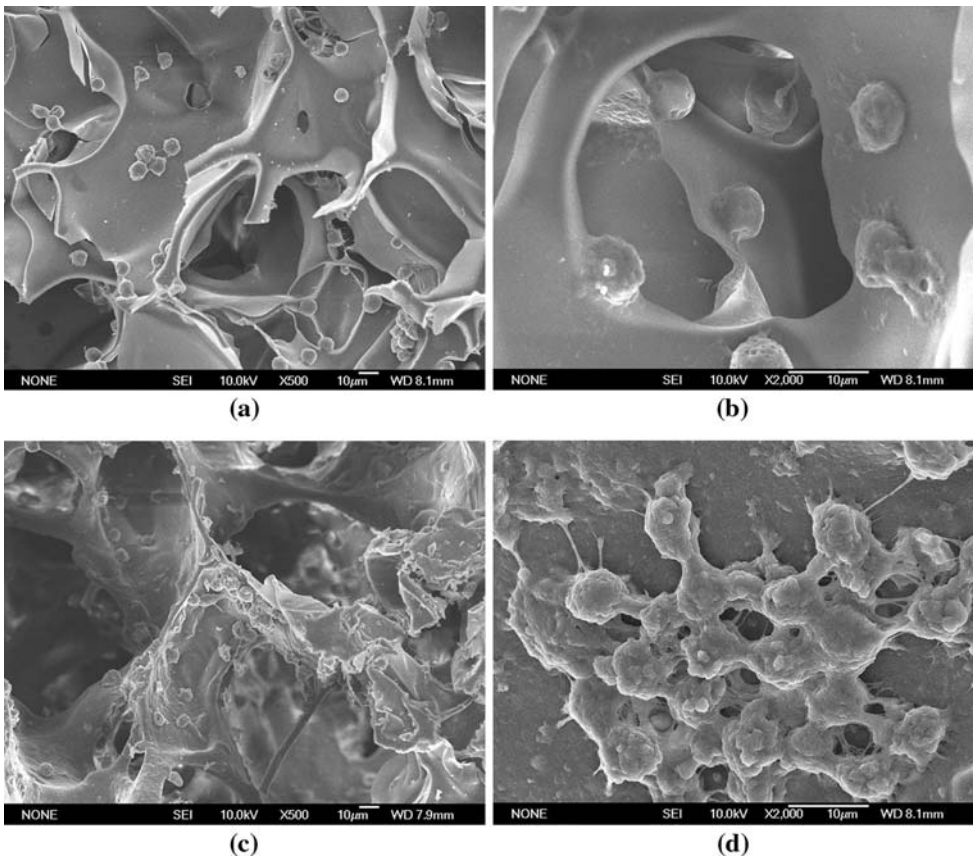

Fig. 5 FESEM micrographs of cells cultured within chitosan scaffolds (CT_0) and TiO_2/chitosan composite ($CT_{0.3}$) scaffolds for 1 d. **a** CT_0, 500×; **b** CT_0, 2000×; **c** $CT_{0.3}$, 500×; **d** $CT_{0.3}$, 2000×

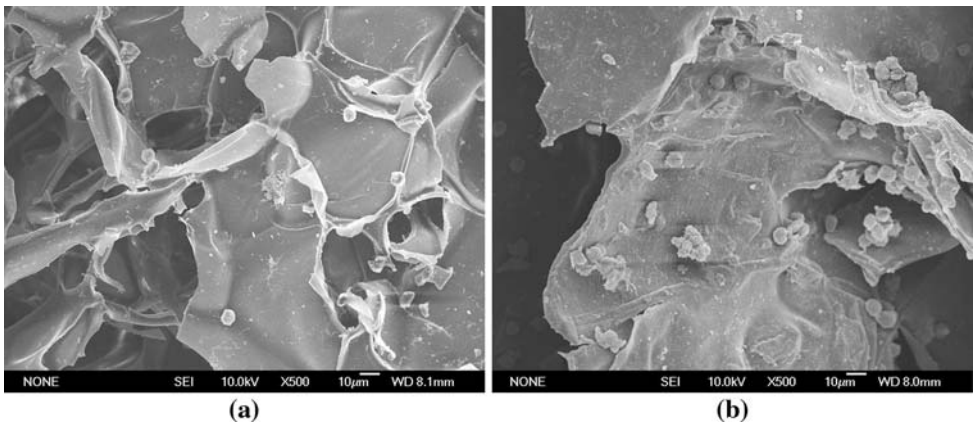

Fig. 6 FESEM micrographs of cells cultured within chitosan scaffolds (CT_0) and TiO_2/chitosan composite ($CT_{0.3}$) scaffolds for 7 d. **a** CT_0, 500×; **b** $CT_{0.3}$, 500×

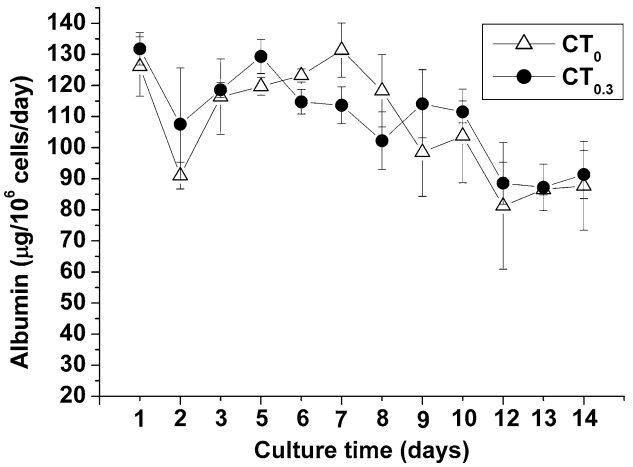

Fig. 7 Albumin secretion rates of HL-7702 cells within chitosan (△) and TiO_2/chitosan composite (●) scaffolds. Each time point represents the mean ± standard derivation of the mean of five experiments

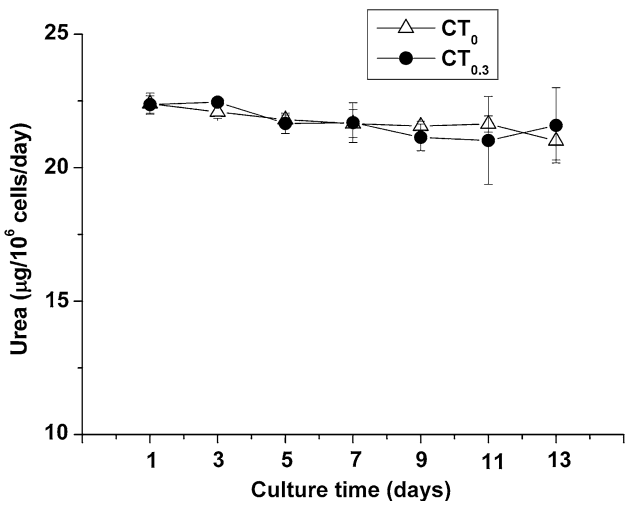

Fig. 8 Urea synthesis rates of HL-7702 cells within the chitosan (△) and TiO_2/chitosan composite (●) scaffolds. Each time point represents the mean ± standard derivation of the mean of five experiments

matrix by the culture medium. In the scaffold with larger pores the hepatocytes spread over larger area, which promotes cellular organization and resembles native cellular environment. This might also influence to give rise to better cell functions [29]. It is well known that multicellular spheroids of hepatocytes with 3D structures maintain hepatic functions to a great extent [30, 31]. In the TiO_2/chitosan composite scaffolds, cells formed spheroid, which could prolong viability in culture and improve liver-specific functions. Cell aggregation is mediated by cell-to-cell adhesion rather than by cell-to-matrix adhesion, and an overly strong cell-to-matrix adhesion would prevent cell aggregation [32]. In the chitosan scaffolds, cells adhered to the matrix, but few cell–cell contacts occurred. In the TiO_2/chitosan composite scaffolds, multicellular spheroids formed, resulting in cell aggregation.

The high level of albumin secretion within the composite scaffold was detected within 24 h of cell seeding and it probably related to spheroid formation. Albumin level throughout the culture period among both the scaffolds slightly decreased with culture time, but it maintained high level as compared to those of normal rat hepatocytes (48 mg/1 × 10^6 cells per day) [33]. This albumin secretion rate has a higher value compared to those of previous in vitro research results [15, 30, 34]. In contrast to albumin secretion, specific urea secretion rate was not dependant on cell aggregation of the constructs [33], and thus, there was no significant difference throughout the culture period. The specific secretion rate of urea from the hepatocyte constructs was less than that reported for normal rat hepatocytes (80–100 mg/1 × 10^6 cells per day), yet it was higher than that reported for hepatocytes seeded on 2D cultures [9, 35]. The decrease in specific rate of albumin and urea secretion with the culture time may be related to a reduction in cell function over time, as was previously shown for hepatocytes seeded on monolayer collagen cultures. From this point, TiO_2/chitosan composite scaffolds were more favorable for retaining HL-7702 cells function.

5 Conclusions

Macroporous TiO_2/chitosan composite scaffolds were successfully prepared by a freeze-drying technique. The TiO_2 powders were uniformly dispersed on the pore walls of the composite scaffolds with lower TiO_2 content. Owing to the addition of TiO_2 powders, the compressive strength of the composite scaffolds was significantly improved. HL-7702 cells adherent to the TiO_2/chitosan composite scaffolds formed multicellular spheroid mostly, exhibiting initial high level of albumin secretion. There was no significant difference for urea synthesis rate between composite scaffold and pure chitosan scaffold during the culture period. HL-7702 cells maintained long-term capability of metabolic activity within the composite scaffolds. Our study indicated that the TiO_2/chitosan composite scaffolds possessed the potential application in liver tissue engineering.

References

1. V. Dixit, Artif. Organs. **18**, 371 (1994)
2. A.T. Gutsche, H. Lo, J. Zurlo, J. Yager, K.W. Leong, Biomaterials **17**, 387 (1996). doi:10.1016/0142-9612(96)85577-3
3. A.G. Mikos, Y. Bao, L.G. Cima, D.E. Ingber, J.P. Vacanti, R. Langer, J. Biomed. Mater. Res. **27**, 183 (1993). doi:10.1002/jbm.820270207
4. A.G. Mikos, A.J. Thorsen, L.A. Czerwonka, Y. Bao, D.N. Winslow, J.P. Vacanti, R. Langer, Polymer (Guildf) **35**, 1068 (1994). doi:10.1016/0032-3861(94)90953-9
5. J.C.Y. Dunn, R.G. Tomkins, M.L. Yarmush, Biotechnol. Prog. **7**, 237 (1991). doi:10.1021/bp00009a007
6. P.V. Moghe, F. Berthiaume, R.M. Ezzell, M. Toner, R.G. Tompkins, M.L. Yarmush, Biomaterials **17**, 373 (1996). doi:10.1016/0142-9612(96)85576-1
7. P.M. Kaufmann, S. Heimrath, B.S. Kim, D.J. Mooney, Cell Transplant. **6**, 463 (1997). doi:10.1016/S0963-6897(97)00052-3
8. D.J. Mooney, K. Sano, P.M. Kaufmann, K. Majahod, B. Schloo, J.P. Vacanti, R. Langer, J. Biomed. Mater. Res. **37**, 413 (1996). doi:10.1002/(SICI)1097-4636(19971205)37:3<413::AID-JBM12>3.0.CO;2-C
9. R. Glicklis, L. Shapiro, R. Agbaria, J.C. Merchuk, S. Cohen, Biotechnol. Bioeng. **67**(3), 344 (2000). doi:10.1002/(SICI)1097-0290(20000205)67:3<344::AID-BIT11>3.0.CO;2-2
10. F. Lim, R.D. Moss, J. Pharm. Sci. **70**(4), 351 (1981). doi:10.1002/jps.2600700402
11. K. Yagi, K. Tsuda, M. Serada, C. Yamada, A. Kondoh, Y. Miura, Artif. Organs. **17**(11), 929 (1993)
12. K. Smentana, Biomaterials **14**, 1046 (1993). doi:10.1016/0142-9612(93)90203-E
13. K. Li, Y. Wang, Z. Miao, D. Xu, Y. Tang, M. Feng, Biotechnol. Lett. **26**, 879 (2004). doi:10.1023/B:bile.0000025896.61490.6d
14. M. Kawase, N. Michibayashi, Y. Nakashima, N. Kurikawa, K. Yagi, T. Mizoguchi, Biol. Pharm. Bull. **20**, 708 (1997)
15. I.-K. Park, J. Yang, H.-J. Jeong, H.-S. Bom, I. Harada, T. Akaike, S.-I. Kim, C.-S. Cho, Biomaterials **24**, 2331 (2003). doi:10.1016/S0142-9612(03)00108-X
16. J. Li, J. Pan, L. Zhang, Y. Yu, Biomaterials **24**, 2317 (2003). doi:10.1016/S0142-9612(03)00048-6
17. D.S. Kommireddy, I. Ichinose, Y.M. Lvov, D.K. Mills, J. Biomed. Nanotechnol. **3**, 286 (2005). doi:10.1166/jbn.2005.046
18. L. Zhao, J. Chang, W. Zhai, J. Biomater. Appl. **19**, 237 (2005). doi:10.1177/0885328205047218
19. S. Buchloh, B. Stieger, P.J. Meier, L. Gauckler, Biomaterials **24**, 2605 (2003). doi:10.1016/S0142-9612(03)00064-4
20. M. Hashimoto, H. Takadama, M. Mizuno, T. Kokubo, J. Mater. Sci.: Mater. Med. **18**, 661 (2007). doi:10.1007/s10856-007-2317-1
21. R. Zhang, P.X. Ma, J. Biomed. Mater. Res. **44**, 446 (1999). doi:10.1002/(SICI)1097-4636(19990315)44:4<446::AID-JBM11>3.0.CO;2-F
22. Y.Y. Hsu, J.D. Gresser, D.J. Trantolo, C.M. Lyons, P.R.J. Gangadharam, D.L. Wise, J. Biomed. Mater. Res. **35**(1), 107 (1997). doi:10.1002/(SICI)1097-4636(199704)35:1<107::AID-JBM11>3.0.CO;2-G
23. Y. Zhang, M. Zhang, J. Mater. Sci.: Mater. Med. **15**, 255 (2004). doi:10.1023/B:JMSM.0000015485.94665.25
24. Y. Yin, F. Ye, J. Cui, F. Zhang, X. Li, K. Yao, J. Biomed. Mater. Res. **67A**, 844 (2003). doi:10.1002/jbm.a.10153
25. S. Li, *Introduction of biomedical materials*, 1st edn. (Wuhan University of Technology Press, Wuhan, 2000), pp. 202–206
26. M. Ito, Y. Hidaka, M. Nakajima, H. Yagasaki, A.H. Kafrawy, J. Biomed. Mater. Res. **45**, 204 (1999). doi:10.1002/(SICI)1097-4636(19990605)45:3<204::AID-JBM7>3.0.CO;2-4
27. C. Selden, M. Khalil, H. Hodgson, Int. J. Artif. Organs. **23**, 774 (2000)
28. L.M. Flendrig, J.W. la Soe, G.G. Jorning, A. Steenbeek, O.T. Karlsen, W.M. Bovee, N.C. Ladiges, A.A. te Velde, R.A. Chamuleau, J. Hepatol. **26**, 1379 (1997). doi:10.1016/S0168-8278(97)80475-8
29. M.E. Hoque, H.-Q. Mao, S. Ramakrishna, J. Biomater. Sci. Polym. Ed. **18**(1), 45 (2007). doi:10.1163/156856207779146088
30. N. Koide, T. Shinji, T. Tanabe, K. Asano, M. Kawaguchi, K. Sakaguchi, Y. Koide, Y. Mori, T. Tsuji, Biochem. Biophys. Res. Commun. **161**, 385 (1989). doi:10.1016/0006-291X(89)91609-4
31. N. Koide, K. Sakaguchi, Y. Koide, K. Asano, M. Kawaguchi, H. Matsushima, T. Takenami, T. Shinji, M. Mori, T. Tsuji, Exp. Cell Res. **186**, 227 (1990). doi:10.1016/0014-4827(90)90300-Y
32. R.C. Bates, N.S. Edwards, J.D. Yates, Crit. Rev. Oncol. Hematol. **36**, 61 (2000). doi:10.1016/S1040-8428(00)00077-9
33. M. Dvir-Ginzberg, I. Gamlieli-Bonshtein, R. Agbaria, S. Cohen, Tissue Eng. **9**(4), 757 (2003). doi:10.1089/107632703768247430
34. B. Feng, J. Weng, B.C. Yang, S.X. Qu, X.D. Zhang, Biomaterials **24**(25), 4663 (2003). doi:10.1016/S0142-9612(03)00366-1
35. G. Catapano, L. De Bartolo, V. Vico, L. Ambrosio, Biomaterials **22**, 659 (2001). doi:10.1016/S0142-9612(00)00228-3